Published for SISSA by Springer

Received: *February 14, 2022*
Revised: *April 1, 2022*
Accepted: *April 8, 2022*
Published: *May 6, 2022*

JHEP05(2022)038

Observation of the doubly charmed baryon decay $\Xi_{cc}^{++} \to \Xi_{c}^{\prime +}\pi^{+}$

The LHCb collaboration

E-mail: wenqian.huang@cern.ch

Abstract: The $\Xi_{cc}^{++} \to \Xi_{c}^{\prime +}\pi^{+}$ decay is observed using proton-proton collisions collected by the LHCb experiment at a centre-of-mass energy of 13 TeV, corresponding to an integrated luminosity of $5.4\,\mathrm{fb}^{-1}$. The $\Xi_{cc}^{++} \to \Xi_{c}^{\prime +}\pi^{+}$ decay is reconstructed partially, where the photon from the $\Xi_{c}^{\prime +} \to \Xi_{c}^{+}\gamma$ decay is not reconstructed and the $pK^{-}\pi^{+}$ final state of the Ξ_{c}^{+} baryon is employed. The $\Xi_{cc}^{++} \to \Xi_{c}^{\prime +}\pi^{+}$ branching fraction relative to that of the $\Xi_{cc}^{++} \to \Xi_{c}^{+}\pi^{+}$ decay is measured to be $1.41 \pm 0.17 \pm 0.10$, where the first uncertainty is statistical and the second systematic.

Keywords: Charm Physics, Flavour Physics, Hadron-Hadron Scattering, Proton-Proton Scattering

ArXiv ePrint: 2202.05648

https://doi.org/10.1007/JHEP05(2022)038

Contents

1 Introduction

The quark model [1–3] predicts the existence of doubly charmed baryons that contain two charm quarks and a light quark (u, d, s), providing ideal systems to test effective theories of quantum chromodynamics (QCD). In 2017, the LHCb collaboration reported the first observation of the doubly charmed baryon Ξ_{cc}^{++} using the decay into the $\Lambda_c^+ K^- \pi^+ \pi^+$ final state, and measured its mass [4].[1] This observation has been confirmed using the $\Xi_{cc}^{++} \to \Xi_c^+ \pi^+$ decay mode [5], as proposed by ref. [6]. The LHCb collaboration also measured the Ξ_{cc}^{++} lifetime [7] and the production rate [8], and established an upper limit for the $\Xi_{cc}^{++} \to D^+ p K^- \pi^+$ decay mode [9]. The Ξ_{cc}^{++} mass has been measured [10] using both the $\Xi_{cc}^{++} \to \Lambda_c^+ K^- \pi^+ \pi^+$ and $\Xi_{cc}^{++} \to \Xi_c^+ \pi^+$ decays.

This paper presents the observation of the $\Xi_{cc}^{++} \to \Xi_c^{\prime +} \pi^+$ decay and the measurement of its branching fraction relative to that of the $\Xi_{cc}^{++} \to \Xi_c^+ \pi^+$ transition,

$$\frac{\mathcal{B}(\Xi_{cc}^{++} \to \Xi_c^{\prime +} \pi^+)}{\mathcal{B}(\Xi_{cc}^{++} \to \Xi_c^+ \pi^+)}, \tag{1.1}$$

using proton-proton (pp) collisions collected by the LHCb experiment at a centre-of-mass energy of 13 TeV, corresponding to an integrated luminosity of 5.4 fb^{-1}. The signal $\Xi_{cc}^{++} \to \Xi_c^{\prime +} \pi^+$ decay is partially reconstructed, with the photon from the $\Xi_c^{\prime +} \to \Xi_c^+ \gamma$ process not reconstructed. The Ξ_c^+ baryon is reconstructed with the $\Xi_c^+ \to p K^- \pi^+$ decay for both the signal and normalisation modes. This measurement can be used to test various theoretical models, by comparing the measured relative branching fraction to theoretical predictions. There is a wide spread in these predicted values, due to several theory assumptions.

[1]The inclusion of charge-conjugate processes is implied throughout.

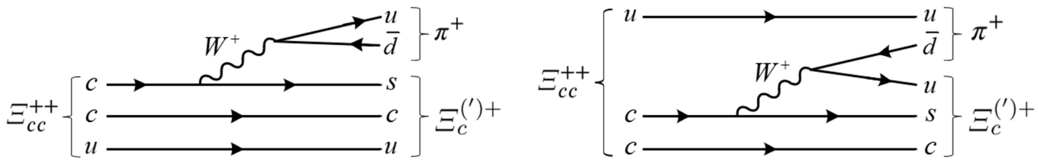

Figure 1. (Left) external and (right) internal W-emission diagrams of the $\Xi_{cc}^{++} \to \Xi_c^{(\prime)+}\pi^+$ decay.

Two topological diagrams contribute to the $\Xi_{cc}^{++} \to \Xi_c^{(\prime)+}\pi^+$ decay amplitude, as shown in figure 1, corresponding to external and internal W-emission. The contribution of the internal W-emission can vary. Including the contribution from the internal W-emission, the relative branching fraction is predicted between 0.81 and 0.83 [11, 12]. Additionally, including the rescattering mechanism between the final-state hadrons, the predicted relative branching fraction varies between 0.44 and 0.70 [13]. When the interference between the external and the internal W-emission contributions for both S- and P-wave amplitudes are considered, the relative branching fraction is predicted to be considerably enhanced at 6.74 [14].

The flavour wave-function symmetry can affect the relative branching ratio. The flavour wave-function of the Ξ_{cc}^{++} and Ξ_c^+ baryons is antisymmetric, while it is symmetric for the $\Xi_c^{\prime+}$ state, which implies that the $\Xi_{cc}^{++} \to \Xi_c^+ X$ transition is flavour symmetric while $\Xi_{cc}^{++} \to \Xi_c^{\prime+} X$ is flavour antisymmetric. As predicted by the Körner-Pati-Woo theorem [15, 16], the internal W-emission amplitude of the $\Xi_{cc}^{++} \to \Xi_c^{\prime+} X$ transition is suppressed due to its flavour antisymmetry. Including the Körner-Pati-Woo theorem, the relative branching fraction is predicted to be 4.33 [17–19] and 4.55 [20].

Finally, two models are considered that approximate the internal structure and the weak-decay of the Ξ_{cc}^{++} state by treating two of the three quarks as a diquark system. The first model assumes a $(cu)c$ configuration, where the single c quark decays and the diquark remains a spectator, leading to a prediction of the relative branching fraction of 0.70 [21]. The second model takes the $(cc)u$ configuration with the diquark system breaking apart, leading to a $(cc)u \to c(su)$ transition and a predicted relative branching fraction of 0.56 ± 0.18 [22] and 0.30 ± 0.24 [22, 23].

The rest of this paper is organised as follows. In section 2, a brief introduction to the LHCb detector and the simulation framework is given. Sections 3 and 4 describe the event selection and the measurement of the $\Xi_{cc}^{++} \to \Xi_c^{\prime+}\pi^+$ branching fraction relative to the $\Xi_{cc}^{++} \to \Xi_c^+\pi^+$ decay. The systematic uncertainties related to this measurement are reported in section 5. Finally, the results are summarized in section 6.

2 Detector and simulation

The LHCb detector [24, 25] is a single-arm forward spectrometer covering the pseudorapidity range $2 < \eta < 5$, designed for the study of particles containing b or c quarks. The detector includes a high-precision tracking system consisting of a silicon-strip vertex detector surrounding the pp interaction region, a large-area silicon-strip detector located upstream of a dipole magnet with a bending power of about 4 Tm, and three stations of silicon-strip detectors and straw drift tubes placed downstream of the magnet. The tracking system provides a measurement of the momentum, p, of charged particles with a relative uncertainty that varies from 0.5% at low momentum to 1.0% at 200 GeV/c. The minimum distance of a track to a primary pp collision vertex, the impact parameter, is measured with a resolution of $(15 + 29/p_{\mathrm{T}})\,\mu\mathrm{m}$, where p_{T} is the component of the momentum transverse to the beam, in GeV/c. Different types of charged hadrons are distinguished using information from two ring-imaging Cherenkov detectors. Photons, electrons and hadrons are identified by a calorimeter system consisting of scintillating-pad and preshower detectors, an electromagnetic and a hadronic calorimeter. Muons are identified by a system composed of alternating layers of iron and multiwire proportional chambers.

The online event selection is performed by a trigger [26], which consists of a hardware stage, based on information from the calorimeter and muon systems, followed by two software stages, which apply partial and full event reconstructions sequentially. At the first software stage one or two tracks with a large impact parameter significance and p_{T} is required. Then an alignment and calibration of the detector is performed in near real-time [27]. This process allows the reconstruction of Ξ_{cc}^{++} decays to be performed entirely in the second stage of the software trigger [28], whose output is used as input to the present analysis.

Simulation samples are used to model the effects of the detector acceptance and to estimate the efficiencies of the selection requirements. In the simulation, pp collisions are generated using Pythia 8 [29, 30] with a specific LHCb configuration [31]. A dedicated generator GenXicc2.0 [32] is used for the Ξ_{cc}^{++} production. Decays of unstable particles are described by EvtGen [33], in which final-state radiation is generated using Photos [34]. The interaction of the generated particles with the detector, and its response, are implemented using the Geant4 toolkit [35]. Fast simulated samples generated with the AmpGen [36, 37] and RapidSim [38] toolkits are also used to study the signal distribution with different amplitude hypotheses and to estimate various background decays that may appear in the data, such as $\Xi_{cc}^{++} \to \Xi_c(2645/2790)^+\pi^+$ decays. Simulated events are generated with a Ξ_{cc}^{++} mass of 3621 MeV/c^2 [10] and a lifetime of 256 fs [7].

3 Event selection

The reconstruction and event selection of the $\Xi_{cc}^{++} \to \Xi_c^{(\prime)+}\pi^+$ decays are the same as in the previous Ξ_{cc}^{++} LHCb analysis [10] except for the trigger requirements. Two positively and one negatively charged tracks, corresponding to the final-state particles of the $\Xi_c^+ \to pK^-\pi^+$ candidate, are required to form a good quality vertex. An additional, positively charged track is combined with the Ξ_c^+ candidate to form a $\Xi_{cc}^{++} \to \Xi_c^{(\prime)+}\pi^+$ candidate with a second good quality vertex. The two vertices and all tracks are required to be detached from any primary pp collision vertex. Particle identification (PID) is required on the four tracks. A multilayer perceptron (MLP) algorithm from the Tmva toolkit [39, 40] is used to improve the signal purity. The MLP algorithm is trained using simulated $\Xi_{cc}^{++} \to \Xi_c^+\pi^+$ events as signal proxy and wrong-sign $\Xi_c^+\pi^-$ combinations in data as background proxy. Variables associated with the Ξ_{cc}^{++} candidates and their decay products are used in the training. The threshold applied to the MLP response is determined by maximising the signal significance

$S/\sqrt{S+B}$, where S and B are the expected yields of signal and background in the signal region of the $\Xi_{cc}^{++} \to \Xi_c^+ \pi^+$ decay, respectively. This MLP working point also works well for the $\Xi_{cc}^{++} \to \Xi_c^{\prime +} \pi^+$ decay.

Compared with the previous analysis [10], the data samples are further split into two disjoint subsamples using information from the hardware trigger. In this way the hardware trigger efficiencies for these two subsamples are well defined. The first contains candidates that are triggered by at least one of the Ξ_c^+ decay products with high transverse energy deposited in the calorimeters, and is referred to as triggered on signal (TOS). The second consists of events that are exclusively triggered by particles unrelated to the signal decay products; these events can be triggered, for example, by the decay products of charmed hadrons produced together with the signal baryon, and are referred to as exclusively triggered independently of signal (TIS).

4 Relative branching fraction measurement

To measure the branching fraction of the signal decay relative to that of the normalisation channel, both the relative signal yields and efficiencies must be determined, as defined below,

$$\frac{\mathcal{B}(\Xi_{cc}^{++} \to \Xi_c^{\prime +} \pi^+)}{\mathcal{B}(\Xi_{cc}^{++} \to \Xi_c^{+} \pi^+)} = \frac{N_{\Xi_c^{\prime +}}}{N_{\Xi_c^{+}}} \times \frac{\epsilon_{\Xi_c^{+}}}{\epsilon_{\Xi_c^{\prime +}}}, \tag{4.1}$$

where $N_{\Xi_c^{(\prime)+}}$ is the signal yield of the $\Xi_{cc}^{++} \to \Xi_c^{(\prime)+} \pi^+$ decay, and $\epsilon_{\Xi_c^{(\prime)+}}$ is the total efficiency for each decay. The relative signal yield is determined by fitting the $\Xi_c^+ \pi^+$ invariant-mass spectrum in the data, and the relative efficiency is determined from fully simulated samples of the signal and normalisation decay modes.

The $\Xi_c^+ \pi^+$ invariant-mass spectrum, separated for TOS and TIS samples, are shown in figure 2. The peaking structure around 3620 MeV/c^2 is due to the $\Xi_{cc}^{++} \to \Xi_c^+ \pi^+$ decay, and the box-like enhancement between 3480 and 3560 MeV/c^2 is due to the $\Xi_{cc}^{++} \to \Xi_c^{\prime +} \pi^+$ decay, shifted down and distorted because of the unreconstructed photon.

An unbinned maximum-likelihood fit is performed simultaneously to the invariant-mass distribution $M(\Xi_c^+ \pi^+) \equiv m(\Xi_c^+ \pi^+) - m(\Xi_c^+) + m_0(\Xi_c^+)$. Here, $m(\Xi_c^+ \pi^+)$ and $m(\Xi_c^+)$ are the reconstructed invariant masses of the Ξ_{cc}^{++} and Ξ_c^+ candidates, and $m_0(\Xi_c^+)$ is the known Ξ_c^+ mass [41].

Four components are considered in the fit model, separately for the TOS and TIS categories. The $\Xi_{cc}^{++} \to \Xi_c^+ \pi^+$ decay is described by a Crystal Ball (CB) function [42], defined as

$$f(x|\alpha, n, \bar{x}, \sigma) = \begin{cases} e^{-\frac{(x-\bar{x})^2}{2\sigma^2}} & \text{for } \frac{x-\bar{x}}{\sigma} > -\alpha \\ \left(\frac{n}{\alpha}\right)^n e^{-\frac{\alpha^2}{2}} \left(\frac{n}{\alpha} - \alpha - \frac{x-\bar{x}}{\sigma}\right)^{-n} & \text{for } \frac{x-\bar{x}}{\sigma} \leqslant -\alpha, \end{cases} \tag{4.2}$$

where $\bar{x}$ is the mean mass and is shared between the TOS and TIS samples and σ is the mass resolution and is varied independently in the two subsamples. The parameters α and n describe the tail caused by the final-state radiation, and are parameterised as a function of the mass resolution as done in ref. [10]. The $\Xi_{cc}^{++} \to \Xi_c^{\prime +} \pi^+$ decay is described by a

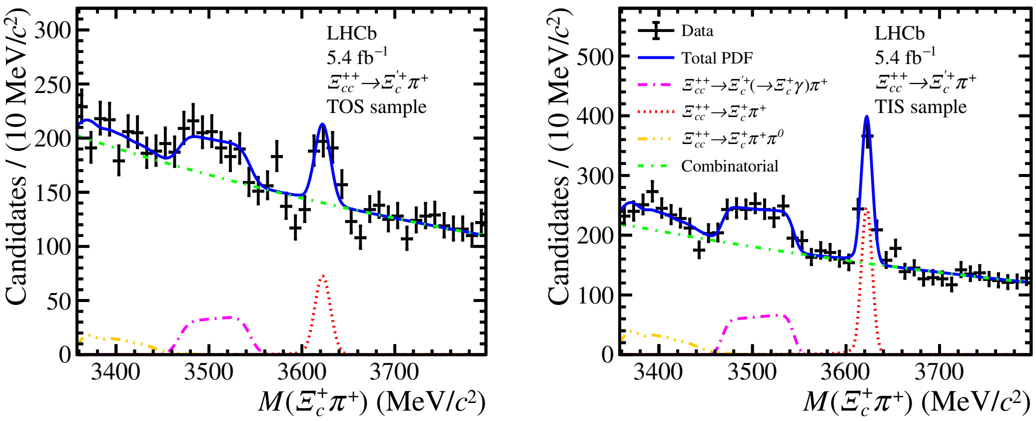

Figure 2. Invariant-mass distribution of the Ξ_{cc}^{++} candidates from the (left) TOS and (right) TIS samples, with the results of the fit overlaid. The $\Xi_{cc}^{++}\to\Xi_c^{\prime+}\pi^+$ component is shown as a purple dashed line, the $\Xi_{cc}^{++}\to\Xi_c^+\pi^+$ component as a red dotted line, the $\Xi_{cc}^{++}\to\Xi_c^+\pi^+\pi^0$ component as a yellow dashed line and the combinatorial component as a green dashed line.

Category	$\Xi_{cc}^{++}\to\Xi_c^{\prime+}\pi^+$	$\Xi_{cc}^{++}\to\Xi_c^+\pi^+$	$N_{\Xi_c^{\prime+}}/N_{\Xi_c^+}$
TOS	262 ± 53	159 ± 32	1.64 ± 0.39
TIS	494 ± 63	379 ± 32	1.30 ± 0.18

Table 1. Yields of the signal and normalisation decay modes, and the relative yields.

limited linear function describing the true mass distribution of the signal convoluted with the Gaussian mass resolution σ. The limited linear function is defined as

$$f\left(x|k,x_{\min},x_{\max}\right)=\begin{cases}k\frac{x-x_{\min}}{x_{\max}-x_{\min}}-\frac{k-1}{2} & \text{for } x_{\min}\leqslant x\leqslant x_{\max}\\ 0 & \text{other,}\end{cases}\tag{4.3}$$

where the lower and upper boundaries $(x_{\min},x_{\max})$ of the function are fixed by the allowed kinematic range, while the slope k is determined from simulation. The distribution of the partially reconstructed background $\Xi_{cc}^{++}\to\Xi_c^+\pi^+\pi^0$ is taken from simulation, where the relative yield between this component and the $\Xi_{cc}^{++}\to\Xi_c^+\pi^+$ decay in the TOS sample is fixed according to that in the TIS sample and the relative efficiencies between these two decays in the simulated TIS and TOS samples. The combinatorial background in each sample is described by an exponential function, with their slopes allowed to vary freely in the fit.

The invariant-mass distribution of the Ξ_{cc}^{++} candidates together with the fit results for the two trigger categories are shown in figure 2. The signal and normalisation yields determined from the fit, along with the relative yields, are listed in table 1, where the quoted uncertainties are statistical only. The statistical significance of the $\Xi_{cc}^{++}\to\Xi_c^{\prime+}\pi^+$ decay is 9.6 standard deviations, obtained by applying a likelihood ratio test to fits with and without the signal component.

Fully simulated samples of the signal and the normalisation modes are used to evaluate the relative efficiencies. For both modes, the kinematic distributions in simulation, including

Source	TOS [%]	TIS [%]
Signal model	4.9	0.8
normalisation model	3.7	3.8
Combinatorial background	0.6	3.1
Partially reconstructed background	3.7	1.5
Mass window	11.0	3.9
Simulated sample size	4.5	3.6
Lifetime and kinematic corrections	0.5	1.8
Hardware trigger	0.0	1.6
Particle identification	0.5	0.7
Sum in quadrature	13.9	7.9

Table 2. Relative systematic uncertainties on the branching fraction ratio $\frac{\mathcal{B}(\Xi_{cc}^{++}\to\Xi_c^{\prime +}\pi^+)}{\mathcal{B}(\Xi_{cc}^{++}\to\Xi_c^{+}\pi^+)}$.

the Ξ_{cc}^{++} transverse momentum and event multiplicity, are weighted to match those in data, separately for the TOS and TIS categories. The background-subtracted distributions in the data are determined with the *sPlot* method [43], using $M(\Xi_c^+\pi^+)$ as discriminating variable in the region between 3570 and 3680 MeV/c^2, where only the $\Xi_{cc}^{++}\to\Xi_c^+\pi^+$ decay and combinatorial background are present. The fit model for these components is the same as described previously. The relative efficiencies are determined to be 1.105 ± 0.050 and 1.029 ± 0.037 for TOS and TIS samples, respectively, where the uncertainties are statistical.

5 Systematic uncertainties

The relative branching fraction measurement has systematic uncertainties arising from determinations of the relative signal yields and efficiencies, as summarised in table 2.

Uncertainties from the determination of the relative signal yields are caused by imperfect modeling of each component in the invariant-mass fit. To estimate such effects, alternative models are used, replacing the corresponding components discussed in section 4, and the changes of the relative signal yields are taken as systematic uncertainties. A template from the fully simulated signal sample is used as an alternative signal, and replaces the limited linear function convoluted with the resolution function, leading to a systematic uncertainty of 4.9% (0.8%) for the TOS (TIS) sample. The alternative model for the normalisation decay mode is a CB function with the tail parameters α and n varied in the fit, leading to a systematic uncertainty of 3.7% (3.8%). For the combinatorial background, a second-order polynomial function is used, and a systematic uncertainty of 0.6% (3.1%) is assigned.

To estimate the uncertainties from partially reconstructed background, the following decay channels are generated and reconstructed with the same final-state particles as the default, using the fast simulation toolkits [36–38], assuming different angular momentum hypotheses (S-, P-, D-wave or a mixture if possible), whereas the additional neutral pion(s), the negatively charged pion and the photon are unreconstructed:

- $\Xi_{cc}^{++}\to\Xi_c^+\rho^+$, $\rho^+\to\pi^+\pi^0$, phase-space and different angular momentum hypotheses;

- $\Xi_{cc}^{++} \to \Xi_c^+\pi^+\pi^0$ without intermediate states;
- $\Xi_{cc}^{++} \to \Xi_c(2645)^+\pi^+,\ \Xi_c(2645)^+ \to \Xi_c^+\pi^0$, with different angular momentum hypotheses;
- $\Xi_{cc}^{+} \to \Xi_c(2645)^0\pi^+,\ \Xi_c(2645)^0 \to \Xi_c^+\pi^-$;
- $\Xi_{cc}^{++} \to \Xi_c(2790)^+\pi^+,\ \Xi_c(2790)^+ \to \Xi_c'^+\pi^0,\ \Xi_c'^+ \to \Xi_c^+\gamma$;
- $\Xi_{cc}^{++} \to \Xi_c(2815)^+\pi^+,\ \Xi_c(2815)^+ \to \Xi_c(2645)^+\pi^0,\ \Xi_c(2645)^+ \to \Xi_c^+\pi^0$.

Including the first two sources, the fits give similar results as the default fit. The statistical significance of the third and fourth decay modes is less than two standard deviations. The $M(\Xi_c^+\pi^+)$ distributions of the last two decay modes are outside the mass window used in this analysis and can be ignored. Including all sources of the partially reconstructed background, the largest deviation from the default relative signal yields is taken as a systematic uncertainty of 3.7% (1.5%).

As the signal decay is partially reconstructed, and there is no low-mass sideband to constrain the background shape in the signal region, uncertainties due to the range of the chosen invariant-mass window are also evaluated. The $M(\Xi_c^+\pi^+)$ upper sideband is primarily combinatorial background, its shape is well described by the default parameterization, therefore, only the effects from the low-mass window boundary are considered. The low-mass window boundary is varied from 3350 to 3450 MeV/c^2, and the largest deviation from the default relative signal yield is taken as a systematic uncertainty, leading to 11.0% (3.9%). Although this is the largest contribution among all the systematic uncertainties, the relative branching fraction is still dominated by the statistical uncertainty.

Three sources of systematic uncertainty arising from the determination of the relative efficiencies are evaluated. First, the uncertainty due to the limited size of the simulated samples contributes 4.5% (3.6%). The second is due to the Ξ_{cc}^{++} lifetime and kinematic corrections to the simulation. The Ξ_{cc}^{++} lifetime [7] is varied within its uncertainty, and the resulting change of the relative efficiency is taken as a systematic uncertainty. For the kinematic corrections, different binning schemes are used to determine the weights, which are varied by one standard deviation. Thus, the uncertainties from both the weighting method and the limited size of the background-subtracted data are considered. The relative uncertainty due to the Ξ_{cc}^{++} lifetime and kinematic corrections to the simulation, is less than 1% for the TOS and 1.8% for the TIS samples. There is an additional photon in the $\Xi_{cc}^{++} \to \Xi_c'^+\pi^+$ decay compared to the normalisation decay, which can pass the photon-related hardware trigger in the TIS category. By excluding such a contribution, the relative efficiency of the TIS category changes by 1.6%, which is taken as a systematic uncertainty. The last contribution arises from uncertainty on the PID efficiency and is studied using calibration samples [44]. The relative uncertainty is found to be less than 1% for both the TOS and TIS samples. As the signal and normalisation decay modes have the same final states and very similar kinematic distributions, other systematic sources, such as the tracking efficiency, mostly cancel in the ratio and are found to be negligible.

6 Results and summary

Including all systematic uncertainties, the measured relative branching fraction in the TOS and TIS samples are $1.81 \pm 0.43 \pm 0.25$ and $1.34 \pm 0.19 \pm 0.11$, respectively, where the first uncertainty is statistical and the second systematic. The combination of the two measurements is performed using the best linear unbiased estimator [45–48]. In the combination, uncertainties arising from the modelling of the signal and normalisation modes, combinatorial and partially reconstructed background, and PID efficiency are assumed to be 100% correlated between the TOS and TIS samples, while the remaining uncertainties are taken to be uncorrelated. The combined result is

$$\frac{\mathcal{B}(\Xi_{cc}^{++} \to \Xi_c'^{+}\pi^+)}{\mathcal{B}(\Xi_{cc}^{++} \to \Xi_c^{+}\pi^+)} = 1.41 \pm 0.17 \pm 0.10.$$

In summary, a new decay mode of the doubly charmed baryon $\Xi_{cc}^{++} \to \Xi_c'^{+}\pi^+$ is observed in a data sample of pp collisions collected by the LHCb experiment at a centre-of-mass energy of $\sqrt{s} = 13\,\text{TeV}$, corresponding to an integrated luminosity of $5.4\,\text{fb}^{-1}$. This is the third observed decay mode of the Ξ_{cc}^{++} baryon following the $\Xi_{cc}^{++} \to \Lambda_c^+ K^- \pi^+ \pi^+$ [4] and $\Xi_{cc}^{++} \to \Xi_c^+ \pi^+$ [5] decays. The relative branching fraction between the $\Xi_{cc}^{++} \to \Xi_c'^{+}\pi^+$ and $\Xi_{cc}^{++} \to \Xi_c^+ \pi^+$ decays is measured for the fist time. The result is not consistent with current theoretical predictions [11, 12, 14, 17–23], and will provide inputs for future calculations.

Acknowledgments

We express our gratitude to our colleagues in the CERN accelerator departments for the excellent performance of the LHC. We thank the technical and administrative staff at the LHCb institutes. We acknowledge support from CERN and from the national agencies: CAPES, CNPq, FAPERJ and FINEP (Brazil); MOST and NSFC (China); CNRS/IN2P3 (France); BMBF, DFG and MPG (Germany); INFN (Italy); NWO (Netherlands); MNiSW and NCN (Poland); MEN/IFA (Romania); MSHE (Russia); MICINN (Spain); SNSF and SER (Switzerland); NASU (Ukraine); STFC (United Kingdom); DOE NP and NSF (U.S.A.). We acknowledge the computing resources that are provided by CERN, IN2P3 (France), KIT and DESY (Germany), INFN (Italy), SURF (Netherlands), PIC (Spain), GridPP (United Kingdom), RRCKI and Yandex LLC (Russia), CSCS (Switzerland), IFIN-HH (Romania), CBPF (Brazil), PL-GRID (Poland) and NERSC (U.S.A.). We are indebted to the communities behind the multiple open-source software packages on which we depend. Individual groups or members have received support from ARC and ARDC (Australia); AvH Foundation (Germany); EPLANET, Marie Skłodowska-Curie Actions and ERC (European Union); A*MIDEX, ANR, IPhU and Labex P2IO, and Région Auvergne-Rhône-Alpes (France); Key Research Program of Frontier Sciences of CAS, CAS PIFI, CAS CCEPP, Fundamental Research Funds for the Central Universities, and Sci. & Tech. Program of Guangzhou (China); RFBR, RSF and Yandex LLC (Russia); GVA, XuntaGal and GENCAT (Spain); the Leverhulme Trust, the Royal Society and UKRI (United Kingdom).

JHEP05(2022)038

References

[1] M. Gell-Mann, *A schematic model of baryons and mesons*, Phys. Lett. **8** (1964) 214 [INSPIRE].

[2] G. Zweig, *An SU_3 model for strong interaction symmetry and its breaking; Version 1*, Tech. Rep. CERN-TH-401, CERN, Geneva (1964).

[3] G. Zweig, *An SU_3 model for strong interaction symmetry and its breaking; Version 2*, Tech. Rep. CERN-TH-412, CERN, Geneva (1964).

[4] LHCb collaboration, *Observation of the doubly charmed baryon Ξ_{cc}^{++}*, Phys. Rev. Lett. **119** (2017) 112001 [arXiv:1707.01621] [INSPIRE].

[5] LHCb collaboration, *First observation of the doubly charmed baryon decay $\Xi_{cc}^{++} \to \Xi_c^{+}\pi^{+}$*, Phys. Rev. Lett. **121** (2018) 162002 [arXiv:1807.01919] [INSPIRE].

[6] F.-S. Yu, H.-Y. Jiang, R.-H. Li, C.-D. Lü, W. Wang and Z.-X. Zhao, *Discovery potentials of doubly charmed baryons*, Chin. Phys. C **42** (2018) 051001 [arXiv:1703.09086] [INSPIRE].

[7] LHCb collaboration, *Measurement of the lifetime of the doubly charmed baryon Ξ_{cc}^{++}*, Phys. Rev. Lett. **121** (2018) 052002 [arXiv:1806.02744] [INSPIRE].

[8] LHCb collaboration, *Measurement of Ξ_{cc}^{++} production in pp collisions at $\sqrt{s} = 13$ TeV*, Chin. Phys. C **44** (2020) 022001 [arXiv:1910.11316] [INSPIRE].

[9] LHCb collaboration, *A search for $\Xi_{cc}^{++} \to D^{+}pK^{-}\pi^{+}$ decays*, JHEP **10** (2019) 124 [arXiv:1905.02421] [INSPIRE].

[10] LHCb collaboration, *Precision measurement of the Ξ_{cc}^{++} mass*, JHEP **02** (2020) 049 [arXiv:1911.08594] [INSPIRE].

[11] N. Sharma and R. Dhir, *Estimates of W-exchange contributions to Ξ_{cc} decays*, Phys. Rev. D **96** (2017) 113006 [arXiv:1709.08217] [INSPIRE].

[12] A.S. Gerasimov and A.V. Luchinsky, *Weak decays of doubly heavy baryons: Decays to a system of π mesons*, Phys. Rev. D **100** (2019) 073015 [arXiv:1905.11740] [INSPIRE].

[13] J.-J. Han, H.-Y. Jiang, W. Liu, Z.-J. Xiao and F.-S. Yu, *Rescattering mechanism of weak decays of double-charm baryons*, Chin. Phys. C **45** (2021) 053105 [arXiv:2101.12019] [INSPIRE].

[14] H.-Y. Cheng, G. Meng, F. Xu and J. Zou, *Two-body weak decays of doubly charmed baryons*, Phys. Rev. D **101** (2020) 034034 [arXiv:2001.04553] [INSPIRE].

[15] J.G. Körner, *Octet behaviour of single-particle matrix elements* $\langle \mathrm{B}'|\mathrm{Hw}|\mathrm{B}\rangle$ *and* $\langle \mathrm{M}'|\mathrm{Hw}|\mathrm{M}\rangle$ *using a weak current-current quark Hamiltonian*, Nucl. Phys. B **25** (1971) 282 [INSPIRE].

[16] J.C. Pati and C.H. Woo, *$\Delta I = \frac{1}{2}$ rule with fermion quarks*, Phys. Rev. D **3** (1971) 2920 [INSPIRE].

[17] T. Gutsche, M.A. Ivanov, J.G. Körner, V.E. Lyubovitskij and Z. Tyulemissov, *Ab initio three-loop calculation of the W-exchange contribution to nonleptonic decays of double charm baryons*, Phys. Rev. D **99** (2019) 056013 [arXiv:1812.09212] [INSPIRE].

[18] T. Gutsche, M.A. Ivanov, J.G. Körner and V.E. Lyubovitskij, *Decay chain information on the newly discovered double charm baryon state Ξ_{cc}^{++}*, Phys. Rev. D **96** (2017) 054013 [arXiv:1708.00703] [INSPIRE].

[19] T. Gutsche, M.A. Ivanov, J.G. Körner, V.E. Lyubovitskij and Z. Tyulemissov, *Analysis of the semileptonic and nonleptonic two-body decays of the double heavy charm baryon states Ξ_{cc}^{++}, Ξ_{cc}^{+} and Ω_{cc}^{+}*, Phys. Rev. D **100** (2019) 114037 [arXiv:1911.10785] [INSPIRE].

[20] M.A. Ivanov, J.G. Körner and V.E. Lyubovitskij, *Nonleptonic decays of doubly charmed baryons*, Phys. Part. Nucl. **51** (2020) 678 [INSPIRE].

[21] W. Wang, F.-S. Yu and Z.-X. Zhao, *Weak decays of doubly heavy baryons: the $1/2 \to 1/2$ case*, Eur. Phys. J. C **77** (2017) 781 [arXiv:1707.02834] [INSPIRE].

[22] H.-W. Ke, F. Lu, X.-H. Liu and X.-Q. Li, *Study on $\Xi_{cc} \to \Xi_c$ and $\Xi_{cc} \to \Xi_c'$ weak decays in the light-front quark model*, Eur. Phys. J. C **80** (2020) 140 [arXiv:1912.01435] [INSPIRE].

[23] Y.-J. Shi, W. Wang and Z.-X. Zhao, *QCD Sum Rules analysis of weak decays of doubly-heavy baryons*, Eur. Phys. J. C **80** (2020) 568 [arXiv:1902.01092] [INSPIRE].

[24] LHCb collaboration, *The LHCb detector at the LHC*, 2008 *JINST* **3** S08005 [INSPIRE].

[25] LHCb collaboration, *LHCb detector performance*, Int. J. Mod. Phys. A **30** (2015) 1530022 [arXiv:1412.6352] [INSPIRE].

[26] R. Aaij et al., *The LHCb trigger and its performance in 2011*, 2013 *JINST* **8** P04022 [arXiv:1211.3055] [INSPIRE].

[27] G. Dujany and B. Storaci, *Real-time alignment and calibration of the LHCb detector in Run II*, J. Phys. Conf. Ser. **664** (2015) 082010 [INSPIRE].

[28] R. Aaij et al., *Tesla: an application for real-time data analysis in High Energy Physics*, Comput. Phys. Commun. **208** (2016) 35 [arXiv:1604.05596] [INSPIRE].

[29] T. Sjöstrand, S. Mrenna and P.Z. Skands, *A brief introduction to PYTHIA 8.1*, Comput. Phys. Commun. **178** (2008) 852 [arXiv:0710.3820] [INSPIRE].

[30] T. Sjöstrand, S. Mrenna and P.Z. Skands, *PYTHIA 6.4 physics and manual*, JHEP **05** (2006) 026 [hep-ph/0603175] [INSPIRE].

[31] LHCb collaboration, *Handling of the generation of primary events in Gauss, the LHCb simulation framework*, J. Phys. Conf. Ser. **331** (2011) 032047 [INSPIRE].

[32] C.-H. Chang, J.-X. Wang and X.-G. Wu, *GENXICC2.0: an upgraded version of the generator for hadronic production of double heavy baryons Ξ_{cc}, Ξ_{bc} and Ξ_{bb}*, Comput. Phys. Commun. **181** (2010) 1144 [arXiv:0910.4462] [INSPIRE].

[33] D.J. Lange, *The EvtGen particle decay simulation package*, Nucl. Instrum. Meth. A **462** (2001) 152 [INSPIRE].

[34] N. Davidson, T. Przedzinski and Z. Was, *PHOTOS interface in C++: Technical and physics documentation*, Comput. Phys. Commun. **199** (2016) 86 [arXiv:1011.0937] [INSPIRE].

[35] GEANT4 collaboration, *Geant4 developments and applications*, IEEE Trans. Nucl. Sci. **53** (2006) 270.

[36] H. Schreiner, H. Pandey, M.D. Sokoloff, B. Hittle, K. Tomko and C. Hasse, *A Python upgrade to the GooFit package for parallel fitting*, EPJ Web Conf. **214** (2019) 05006 [INSPIRE].

[37] T. Evans, *AmpGen, in preparation*, https://github.com/GooFit/AmpGen.

JHEP05(2022)038

[38] G.A. Cowan, D.C. Craik and M.D. Needham, *RapidSim: an application for the fast simulation of heavy-quark hadron decays*, *Comput. Phys. Commun.* **214** (2017) 239 [arXiv:1612.07489] [INSPIRE].

[39] H. Voss, A. Höcker, J. Stelzer and F. Tegenfeldt, *TMVA — toolkit for multivariate data analysis with ROOT*, *PoS* **ACAT** (2007) 040 [INSPIRE].

[40] A. Höcker et al., *TMVA 4 — toolkit for multivariate data analysis with ROOT*, users guide, physics/0703039 [INSPIRE].

[41] Particle Data Group collaboration, *Review of particle physics*, *PTEP* **2020** (2020) 083C01 [INSPIRE].

[42] T. Skwarnicki, *A study of the radiative cascade transitions between the Upsilon-prime and Upsilon resonances*, Ph.D. thesis, Institute of Nuclear Physics, Krakow, Poland (1986).

[43] M. Pivk and F.R. Le Diberder, *sPlot: a statistical tool to unfold data distributions*, *Nucl. Instrum. Meth. A* **555** (2005) 356 [physics/0402083] [INSPIRE].

[44] R. Aaij et al., *Selection and processing of calibration samples to measure the particle identification performance of the LHCb experiment in Run 2*, *EPJ Tech. Instrum.* **6** (2019) 1 [arXiv:1803.00824] [INSPIRE].

[45] L. Lyons, D. Gibaut and P. Clifford, *How to combine correlated estimates of a single physical quantity*, *Nucl. Instrum. Meth. A* **270** (1988) 110 [INSPIRE].

[46] A. Valassi, *Combining correlated measurements of several different physical quantities*, *Nucl. Instrum. Meth. A* **500** (2003) 391 [INSPIRE].

[47] R. Nisius, *BLUE: combining correlated estimates of physics observables within ROOT using the Best Linear Unbiased Estimate method*, arXiv:2001.10310 [INSPIRE].

[48] R. Nisius, *On the combination of correlated estimates of a physics observable*, *Eur. Phys. J. C* **74** (2014) 3004 [arXiv:1402.4016] [INSPIRE].

The LHCb collaboration

R. Aaij[32], A.S.W. Abdelmotteleb[56], C. Abellán Beteta[50], F. Abudinén[56], T. Ackernley[60], B. Adeva[46], M. Adinolfi[54], H. Afsharnia[9], C. Agapopoulou[13], C.A. Aidala[87], S. Aiola[25], Z. Ajaltouni[9], S. Akar[65], J. Albrecht[15], F. Alessio[48], M. Alexander[59], A. Alfonso Albero[45], Z. Aliouche[62], G. Alkhazov[38], P. Alvarez Cartelle[55], S. Amato[2], J.L. Amey[54], Y. Amhis[11], L. An[48], L. Anderlini[22], M. Andersson[50], A. Andreianov[38], M. Andreotti[21], D. Ao[6], F. Archilli[17], A. Artamonov[44], M. Artuso[68], K. Arzymatov[42], E. Aslanides[10], M. Atzeni[50], B. Audurier[12], S. Bachmann[17], M. Bachmayer[49], J.J. Back[56], P. Baladron Rodriguez[46], V. Balagura[12], W. Baldini[21], J. Baptista de Souza Leite[1], M. Barbetti[22,h], R.J. Barlow[62], S. Barsuk[11], W. Barter[61], M. Bartolini[55], F. Baryshnikov[83], J.M. Basels[14], G. Bassi[29], B. Batsukh[4], A. Battig[15], A. Bay[49], A. Beck[56], M. Becker[15], F. Bedeschi[29], I. Bediaga[1], A. Beiter[68], V. Belavin[42], S. Belin[46], V. Bellee[50], K. Belous[44], I. Belov[40], I. Belyaev[41], G. Bencivenni[23], E. Ben-Haim[13], A. Berezhnoy[40], R. Bernet[50], D. Berninghoff[17], H.C. Bernstein[68], C. Bertella[62], A. Bertolin[28], C. Betancourt[50], F. Betti[48], Ia. Bezshyiko[50], S. Bhasin[54], J. Bhom[35], L. Bian[73], M.S. Bieker[15], N.V. Biesuz[21], S. Bifani[53], P. Billoir[13], A. Biolchini[32], M. Birch[61], F.C.R. Bishop[55], A. Bitadze[62], A. Bizzeti[22,l], M. Bjørn[63], M.P. Blago[55], T. Blake[56], F. Blanc[49], S. Blusk[68], D. Bobulska[59], J.A. Boelhauve[15], O. Boente Garcia[46], T. Boettcher[65], A. Boldyrev[82], A. Bondar[43], N. Bondar[38,48], S. Borghi[62], M. Borisyak[42], M. Borsato[17], J.T. Borsuk[35], S.A. Bouchiba[49], T.J.V. Bowcock[60,48], A. Boyer[48], C. Bozzi[21], M.J. Bradley[61], S. Braun[66], A. Brea Rodriguez[46], J. Brodzicka[35], A. Brossa Gonzalo[56], D. Brundu[27], A. Buonaura[50], L. Buonincontri[28], A.T. Burke[62], C. Burr[48], A. Bursche[72], A. Butkevich[39], J.S. Butter[32], J. Buytaert[48], W. Byczynski[48], S. Cadeddu[27], H. Cai[73], R. Calabrese[21,g], L. Calefice[15,13], S. Cali[23], R. Calladine[53], M. Calvi[26,k], M. Calvo Gomez[85], P. Camargo Magalhaes[54], P. Campana[23], A.F. Campoverde Quezada[6], S. Capelli[26,k], L. Capriotti[20,e], A. Carbone[20,e], G. Carboni[31,q], R. Cardinale[24,i], A. Cardini[27], I. Carli[4], P. Carniti[26,k], L. Carus[14], K. Carvalho Akiba[32], A. Casais Vidal[46], R. Caspary[17], G. Casse[60], M. Cattaneo[48], G. Cavallero[48], S. Celani[49], J. Cerasoli[10], D. Cervenkov[63], A.J. Chadwick[60], M.G. Chapman[54], M. Charles[13], Ph. Charpentier[48], C.A. Chavez Barajas[60], M. Chefdeville[8], C. Chen[3], S. Chen[4], A. Chernov[35], V. Chobanova[46], S. Cholak[49], M. Chrzaszcz[35], A. Chubykin[38], V. Chulikov[38], P. Ciambrone[23], M.F. Cicala[56], X. Cid Vidal[46], G. Ciezarek[48], P.E.L. Clarke[58], M. Clemencic[48], H.V. Cliff[55], J. Closier[48], J.L. Cobbledick[62], V. Coco[48], J.A.B. Coelho[11], J. Cogan[10], E. Cogneras[9], L. Cojocariu[37], P. Collins[48], T. Colombo[48], L. Congedo[19,d], A. Contu[27], N. Cooke[53], G. Coombs[59], I. Corredoira [46], G. Corti[48], C.M. Costa Sobral[56], B. Couturier[48], D.C. Craik[64], J. Crkovská[67], M. Cruz Torres[1], R. Currie[58], C.L. Da Silva[67], S. Dadabaev[83], L. Dai[71], E. Dall'Occo[15], J. Dalseno[46], C. D'Ambrosio[48], A. Danilina[41], P. d'Argent[48], A. Dashkina[83], J.E. Davies[62], A. Davis[62], O. De Aguiar Francisco[62], K. De Bruyn[79], S. De Capua[62], M. De Cian[49], U. De Freitas Carneiro Da Graca[1], E. De Lucia[23], J.M. De Miranda[1], L. De Paula[2], M. De Serio[19,d], D. De Simone[50], P. De Simone[23], F. De Vellis[15], J.A. de Vries[80], C.T. Dean[67], F. Debernardis[19,d], D. Decamp[8], V. Dedu[10], L. Del Buono[13], B. Delaney[55], H.-P. Dembinski[15], V. Denysenko[50], D. Derkach[82], O. Deschamps[9], F. Dettori[27,f], B. Dey[77], A. Di Cicco[23], P. Di Nezza[23], S. Didenko[83], L. Dieste Maronas[46], S. Ding[68], V. Dobishuk[52], C. Dong[3], A.M. Donohoe[18], F. Dordei[27], A.C. dos Reis[1], L. Douglas[59], A. Dovbnya[51], A.G. Downes[8], M.W. Dudek[35], L. Dufour[48], V. Duk[78], P. Durante[48], J.M. Durham[67], D. Dutta[62], A. Dziurda[35], A. Dzyuba[38], S. Easo[57], U. Egede[69], V. Egorychev[41], S. Eidelman[43,u,†], S. Eisenhardt[58], S. Ek-In[49], L. Eklund[86], S. Ely[68], A. Ene[37], E. Epple[67], S. Escher[14], J. Eschle[50], S. Esen[50], T. Evans[62], L.N. Falcao[1], Y. Fan[6], B. Fang[73], S. Farry[60], D. Fazzini[26,k], M. Féo[48], A. Fernandez Prieto[46], A.D. Fernez[66], F. Ferrari[20], L. Ferreira Lopes[49], F. Ferreira Rodrigues[2], S. Ferreres Sole[32], M. Ferrillo[50], M. Ferro-Luzzi[48], S. Filippov[39], R.A. Fini[19], M. Fiorini[21,g], M. Firlej[34], K.M. Fischer[63], D.S. Fitzgerald[87], C. Fitzpatrick[62], T. Fiutowski[34], A. Fkiaras[48], F. Fleuret[12], M. Fontana[13], F. Fontanelli[24,i], R. Forty[48], D. Foulds-Holt[55], V. Franco Lima[60], M. Franco Sevilla[66], M. Frank[48], E. Franzoso[21], G. Frau[17], C. Frei[48], D.A. Friday[59], J. Fu[6], Q. Fuehring[15], E. Gabriel[32], G. Galati[19,d], A. Gallas Torreira[46], D. Galli[20,e], S. Gambetta[58,48], Y. Gan[3], M. Gandelman[2], P. Gandini[25], Y. Gao[5], M. Garau[27], L.M. Garcia Martin[56], P. Garcia Moreno[45], J. García Pardiñas[26,k], B. Garcia Plana[46], F.A. Garcia Rosales[12], L. Garrido[45], C. Gaspar[48], R.E. Geertsema[32], D. Gerick[17], L.L. Gerken[15], E. Gersabeck[62], M. Gersabeck[62], T. Gershon[56], L. Giambastiani[28], V. Gibson[55], H.K. Giemza[36], A.L. Gilman[63], M. Giovannetti[23,q], A. Gioventù[46], P. Gironella Gironell[45], C. Giugliano[21], K. Gizdov[58], E.L. Gkougkousis[48], V.V. Gligorov[13,48], C. Göbel[70], E. Golobardes[85], D. Golubkov[41], A. Golutvin[61,83], A. Gomes[1,a], S. Gomez Fernandez[45], F. Goncalves Abrantes[63], M. Goncerz[35], G. Gong[3], P. Gorbounov[41], I.V. Gorelov[40], C. Gotti[26], J.P. Grabowski[17], T. Grammatico[13], L.A. Granado Cardoso[48], E. Graugés[45], E. Graverini[49], G. Graziani[22], A. Grecu[37], L.M. Greeven[32], N.A. Grieser[4], L. Grillo[62], S. Gromov[83], B.R. Gruberg Cazon[63], C. Gu[3], M. Guarise[21], M. Guittiere[11], P. A. Günther[17], E. Gushchin[39], A. Guth[14], Y. Guz[44], T. Gys[48], T. Hadavizadeh[69], G. Haefeli[49], C. Haen[48], J. Haimberger[48], S.C. Haines[55], T. Halewood-leagas[60], P.M. Hamilton[66], J.P. Hammerich[60], Q. Han[7], X. Han[17], E.B. Hansen[62], S. Hansmann-Menzemer[17,48], N. Harnew[63], T. Harrison[60], C. Hasse[48], M. Hatch[48], J. He[6,b], K. Heijhoff[32], K. Heinicke[15], R.D.L. Henderson[69,56], A.M. Hennequin[64], K. Hennessy[60], L. Henry[48], J. Heuel[14], A. Hicheur[2], D. Hill[49], M. Hilton[62], S.E. Hollitt[15], R. Hou[7], Y. Hou[8], J. Hu[17], J. Hu[72], W. Hu[7], X. Hu[3], W. Huang[6], X. Huang[73], W. Hulsbergen[32], R.J. Hunter[56], M. Hushchyn[82], D. Hutchcroft[60], D. Hynds[32], P. Ibis[15], M. Idzik[34], D. Ilin[38], P. Ilten[65], A. Inglessi[38], A. Iniukhin[82], A. Ishteev[83], K. Ivshin[38], R. Jacobsson[48], H. Jage[14], S. Jakobsen[48], E. Jans[32], B.K. Jashal[47], A. Jawahery[66], V. Jevtic[15], X. Jiang[4], M. John[63], D. Johnson[64], C.R. Jones[55], T.P. Jones[56], B. Jost[48], N. Jurik[48], S. Kandybei[51], Y. Kang[3], M. Karacson[48], D. Karpenkov[83], M. Karpov[82], J.W. Kautz[65], F. Keizer[48], D.M. Keller[68], M. Kenzie[56], T. Ketel[33], B. Khanji[15], A. Kharisova[84], S. Kholodenko[44,83], T. Kirn[14], V.S. Kirsebom[49], O. Kitouni[64], S. Klaver[33], N. Kleijne[29], K. Klimaszewski[36], M.R. Kmiec[36], S. Koliiev[52], A. Kondybayeva[83], A. Konoplyannikov[41], P. Kopciewicz[34], R. Kopecna[17], P. Koppenburg[32], M. Korolev[40], I. Kostiuk[32,52], O. Kot[52], S. Kotriakhova[21,38], A. Kozachuk[40], P. Kravchenko[38], L. Kravchuk[39], R.D. Krawczyk[48], M. Kreps[56], S. Kretzschmar[14], P. Krokovny[43,u], W. Krupa[34], W. Krzemien[36], J. Kubat[17], M. Kucharczyk[35], V. Kudryavtsev[43,u], H.S. Kuindersma[32,33], G.J. Kunde[67], T. Kvaratskheliya[41], D. Lacarrere[48], G. Lafferty[62], A. Lai[27], A. Lampis[27], D. Lancierini[50], J.J. Lane[62], R. Lane[54], G. Lanfranchi[23], C. Langenbruch[14], J. Langer[15], O. Lantwin[83], T. Latham[56], F. Lazzari[29], R. Le Gac[10], S.H. Lee[87], R. Lefèvre[9], A. Leflat[40], S. Legotin[83], O. Leroy[10], T. Lesiak[35], B. Leverington[17], H. Li[72], P. Li[17], S. Li[7], Y. Li[4], Z. Li[68], X. Liang[68], T. Lin[57], R. Lindner[48], V. Lisovskyi[15], R. Litvinov[27], G. Liu[72], H. Liu[6], Q. Liu[6], S. Liu[4], A. Lobo Salvia[45], A. Loi[27], R. Lollini[78], J. Lomba Castro[46], I. Longstaff[59], J.H. Lopes[2], S. López Soliño[46], G.H. Lovell[55], Y. Lu[4], C. Lucarelli[22,h], D. Lucchesi[28,m], S. Luchuk[39], M. Lucio Martinez[32], V. Lukashenko[32,52], Y. Luo[3], A. Lupato[62], E. Luppi[21,g], O. Lupton[56], A. Lusiani[29,n], X. Lyu[6], L. Ma[4], R. Ma[6], S. Maccolini[20], F. Machefert[11], F. Maciuc[37], V. Macko[49], P. Mackowiak[15], S. Maddrell-Mander[54], L.R. Madhan Mohan[54], O. Maev[38], A. Maevskiy[82], D. Maisuzenko[38], M.W. Majewski[34], J.J. Malczewski[35], S. Malde[63], B. Malecki[35], A. Malinin[81], T. Maltsev[43,u], H. Malygina[17], G. Manca[27,f], G. Mancinelli[10], D. Manuzzi[20], C.A. Manzari[50], D. Marangotto[25,j], J. Maratas[9,s], J.F. Marchand[8], U. Marconi[20], S. Mariani[22,h], C. Marin Benito[48], M. Marinangeli[49], J. Marks[17], A.M. Marshall[54], P.J. Marshall[60], G. Martelli[78], G. Martellotti[30], L. Martinazzoli[48,k], M. Martinelli[26,k], D. Martinez Santos[46], F. Martinez Vidal[47], A. Massafferri[1], M. Materok[14], R. Matev[48], A. Mathad[50], V. Matiunin[41], C. Matteuzzi[26], K.R. Mattioli[87], A. Mauri[32], E. Maurice[12], J. Mauricio[45], M. Mazurek[48],

M. McCann[61], L. Mcconnell[18], T.H. Mcgrath[62], N.T. Mchugh[59], A. McNab[62], R. McNulty[18], J.V. Mead[60], B. Meadows[65], G. Meier[15], D. Melnychuk[36], S. Meloni[26,k], M. Merk[32,80], A. Merli[25,j], L. Meyer Garcia[2], M. Mikhasenko[75,c], D.A. Milanes[74], E. Millard[56], M. Milovanovic[48], M.-N. Minard[8], A. Minotti[26,k], S.E. Mitchell[58], B. Mitreska[62], D.S. Mitzel[15], A. Mödden [15], R.A. Mohammed[63], R.D. Moise[61], S. Mokhnenko[82], T. Mombächer[46], I.A. Monroy[74], S. Monteil[9], M. Morandin[28], G. Morello[23], M.J. Morello[29,n], J. Moron[34], A.B. Morris[75], A.G. Morris[56], R. Mountain[68], H. Mu[3], F. Muheim[58], M. Mulder[79], K. Müller[50], C.H. Murphy[63], D. Murray[62], R. Murta[61], P. Muzzetto[27], P. Naik[54], T. Nakada[49], R. Nandakumar[57], T. Nanut[48], I. Nasteva[2], M. Needham[58], N. Neri[25,j], S. Neubert[75], N. Neufeld[48], R. Newcombe[61], E.M. Niel[49], S. Nieswand[14], N. Nikitin[40], N.S. Nolte[64], C. Normand[8], C. Nunez[87], A. Oblakowska-Mucha[34], V. Obraztsov[44], T. Oeser[14], D.P. O'Hanlon[54], S. Okamura[21], R. Oldeman[27,f], F. Oliva[58], M.E. Olivares[68], C.J.G. Onderwater[79], R.H. O'Neil[58], J.M. Otalora Goicochea[2], T. Ovsiannikova[41], P. Owen[50], A. Oyanguren[47], O. Ozcelik[58], K.O. Padeken[75], B. Pagare[56], P.R. Pais[48], T. Pajero[63], A. Palano[19], M. Palutan[23], Y. Pan[62], G. Panshin[84], A. Papanestis[57], M. Pappagallo[19,d], L.L. Pappalardo[21], C. Pappenheimer[65], W. Parker[66], C. Parkes[62], B. Passalacqua[21], G. Passaleva[22], A. Pastore[19], M. Patel[61], C. Patrignani[20,e], C.J. Pawley[80], A. Pearce[48,57], A. Pellegrino[32], M. Pepe Altarelli[48], S. Perazzini[20], D. Pereima[41], A. Pereiro Castro[46], P. Perret[9], M. Petric[59,48], K. Petridis[54], A. Petrolini[24,i], A. Petrov[81], S. Petrucci[58], M. Petruzzo[25], T.T.H. Pham[68], A. Philippov[42], R. Piandani[6], L. Pica[29,n], M. Piccini[78], B. Pietrzyk[8], G. Pietrzyk[11], M. Pili[63], D. Pinci[30], F. Pisani[48], M. Pizzichemi[26,48,k], Resmi P.K[10], V. Placinta[37], J. Plews[53], M. Plo Casasus[46], F. Polci[13,48], M. Poli Lener[23], M. Poliakova[68], A. Poluektov[10], N. Polukhina[83,t], I. Polyakov[68], E. Polycarpo[2], S. Ponce[48], D. Popov[6,48], S. Popov[42], S. Poslavskii[44], K. Prasanth[35], L. Promberger[48], C. Prouve[46], V. Pugatch[52], V. Puill[11], G. Punzi[29,o], H. Qi[3], W. Qian[6], N. Qin[3], R. Quagliani[49], N.V. Raab[18], R.I. Rabadan Trejo[6], B. Rachwal[34], J.H. Rademacker[54], R. Rajagopalan[68], M. Rama[29], M. Ramos Pernas[56], M.S. Rangel[2], F. Ratnikov[42,82], G. Raven[33,48], M. Reboud[8], F. Redi[48], F. Reiss[62], C. Remon Alepuz[47], Z. Ren[3], V. Renaudin[63], R. Ribatti[29], A.M. Ricci[27], S. Ricciardi[57], K. Rinnert[60], P. Robbe[11], G. Robertson[58], A.B. Rodrigues[49], E. Rodrigues[60], J.A. Rodriguez Lopez[74], E.R.R. Rodriguez Rodriguez[46], A. Rollings[63], P. Roloff[48], V. Romanovskiy[44], M. Romero Lamas[46], A. Romero Vidal[46], J.D. Roth[87], M. Rotondo[23], M.S. Rudolph[68], T. Ruf[48], R.A. Ruiz Fernandez[46], J. Ruiz Vidal[47], A. Ryzhikov[82], J. Ryzka[34], J.J. Saborido Silva[46], N. Sagidova[38], N. Sahoo[53], B. Saitta[27,f], M. Salomoni[48], C. Sanchez Gras[32], I. Sanderswood[47], R. Santacesaria[30], C. Santamarina Rios[46], M. Santimaria[23], E. Santovetti[31,q], D. Saranin[83], G. Sarpis[14], M. Sarpis[75], A. Sarti[30], C. Satriano[30,p], A. Satta[31], M. Saur[15], D. Savrina[41,40], H. Sazak[9], L.G. Scantlebury Smead[63], A. Scarabotto[13], S. Schael[14], S. Scherl[60], M. Schiller[59], H. Schindler[48], M. Schmelling[16], B. Schmidt[48], S. Schmitt[14], O. Schneider[49], A. Schopper[48], M. Schubiger[32], S. Schulte[49], M.H. Schune[11], R. Schwemmer[48], B. Sciascia[23,48], S. Sellam[46], A. Semennikov[41], M. Senghi Soares[33], A. Sergi[24,i], N. Serra[50], L. Sestini[28], A. Seuthe[15], Y. Shang[5], D.M. Shangase[87], M. Shapkin[44], I. Shchemerov[83], L. Shchutska[49], T. Shears[60], L. Shekhtman[43,u], Z. Shen[5], S. Sheng[4], V. Shevchenko[81], E.B. Shields[26,k], Y. Shimizu[11], E. Shmanin[83], J.D. Shupperd[68], B.G. Siddi[21], R. Silva Coutinho[50], G. Simi[28], S. Simone[19,d], M. Singla[69], N. Skidmore[62], R. Skuza[17], T. Skwarnicki[68], M.W. Slater[53], I. Slazyk[21,g], J.C. Smallwood[63], J.G. Smeaton[55], E. Smith[50], M. Smith[61], A. Snoch[32], L. Soares Lavra[9], M.D. Sokoloff[65], F.J.P. Soler[59], A. Solovev[38], I. Solovyev[38], F.L. Souza De Almeida[2], B. Souza De Paula[2], B. Spaan[15], E. Spadaro Norella[25,j], P. Spradlin[59], F. Stagni[48], M. Stahl[65], S. Stahl[48], S. Stanislaus[63], O. Steinkamp[50,83], O. Stenyakin[44], H. Stevens[15], S. Stone[68,48,†], D. Strekalina[83], F. Suljik[63], J. Sun[27], L. Sun[73], Y. Sun[66], P. Svihra[62], P.N. Swallow[53], K. Swientek[34], A. Szabelski[36], T. Szumlak[34], M. Szymanski[48], S. Taneja[62], A.R. Tanner[54], M.D. Tat[63], A. Terentev[83], F. Teubert[48], E. Thomas[48], D.J.D. Thompson[53], K.A. Thomson[60],

H. Tilquin[61], V. Tisserand[9], S. T'Jampens[8], M. Tobin[4], L. Tomassetti[21,g], X. Tong[5], D. Torres Machado[1], D.Y. Tou[3], E. Trifonova[83], S.M. Trilov[54], C. Trippl[49], G. Tuci[6], A. Tully[49], N. Tuning[32,48], A. Ukleja[36], D.J. Unverzagt[17], E. Ursov[83], A. Usachov[32], A. Ustyuzhanin[42,82], U. Uwer[17], A. Vagner[84], V. Vagnoni[20], A. Valassi[48], G. Valenti[20], N. Valls Canudas[85], M. van Beuzekom[32], M. Van Dijk[49], H. Van Hecke[67], E. van Herwijnen[83], M. van Veghel[79], R. Vazquez Gomez[45], P. Vazquez Regueiro[46], C. Vázquez Sierra[48], S. Vecchi[21], J.J. Velthuis[54], M. Veltri[22,r], A. Venkateswaran[68], M. Veronesi[32], M. Vesterinen[56], D. Vieira[65], M. Vieites Diaz[49], H. Viemann[76], X. Vilasis-Cardona[85], E. Vilella Figueras[60], A. Villa[20], P. Vincent[13], F.C. Volle[11], D. Vom Bruch[10], A. Vorobyev[38], V. Vorobyev[43,u], N. Voropaev[38], K. Vos[80], R. Waldi[17], J. Walsh[29], C. Wang[17], J. Wang[5], J. Wang[4], J. Wang[3], J. Wang[73], M. Wang[3], R. Wang[54], Y. Wang[7], Z. Wang[50], Z. Wang[3], Z. Wang[6], J.A. Ward[56,69], N.K. Watson[53], D. Websdale[61], C. Weisser[64], B.D.C. Westhenry[54], D.J. White[62], M. Whitehead[54], A.R. Wiederhold[56], D. Wiedner[15], G. Wilkinson[63], M. K. Wilkinson[68], I. Williams[55], M. Williams[64], M.R.J. Williams[58], F.F. Wilson[57], W. Wislicki[36], M. Witek[35], L. Witola[17], G. Wormser[11], S.A. Wotton[55], H. Wu[68], K. Wyllie[48], Z. Xiang[6], D. Xiao[7], Y. Xie[7], A. Xu[5], J. Xu[6], L. Xu[3], M. Xu[56], Q. Xu[6], Z. Xu[9], Z. Xu[6], D. Yang[3], S. Yang[6], Y. Yang[6], Z. Yang[5], Z. Yang[66], Y. Yao[68], L.E. Yeomans[60], H. Yin[7], J. Yu[71], X. Yuan[68], O. Yushchenko[44], E. Zaffaroni[49], M. Zavertyaev[16,t], M. Zdybal[35], O. Zenaiev[48], M. Zeng[3], D. Zhang[7], L. Zhang[3], S. Zhang[71], S. Zhang[5], Y. Zhang[5], Y. Zhang[63], A. Zharkova[83], A. Zhelezov[17], Y. Zheng[6], T. Zhou[5], X. Zhou[6], Y. Zhou[6], V. Zhovkovska[11], X. Zhu[3], X. Zhu[7], Z. Zhu[6], V. Zhukov[14,40], Q. Zou[4], S. Zucchelli[20,e], D. Zuliani[28], G. Zunica[62].

[1] *Centro Brasileiro de Pesquisas Físicas (CBPF), Rio de Janeiro, Brazil*
[2] *Universidade Federal do Rio de Janeiro (UFRJ), Rio de Janeiro, Brazil*
[3] *Center for High Energy Physics, Tsinghua University, Beijing, China*
[4] *Institute Of High Energy Physics (IHEP), Beijing, China*
[5] *School of Physics State Key Laboratory of Nuclear Physics and Technology, Peking University, Beijing, China*
[6] *University of Chinese Academy of Sciences, Beijing, China*
[7] *Institute of Particle Physics, Central China Normal University, Wuhan, Hubei, China*
[8] *Univ. Savoie Mont Blanc, CNRS, IN2P3-LAPP, Annecy, France*
[9] *Université Clermont Auvergne, CNRS/IN2P3, LPC, Clermont-Ferrand, France*
[10] *Aix Marseille Univ, CNRS/IN2P3, CPPM, Marseille, France*
[11] *Université Paris-Saclay, CNRS/IN2P3, IJCLab, Orsay, France*
[12] *Laboratoire Leprince-Ringuet, CNRS/IN2P3, Ecole Polytechnique, Institut Polytechnique de Paris, Palaiseau, France*
[13] *LPNHE, Sorbonne Université, Paris Diderot Sorbonne Paris Cité, CNRS/IN2P3, Paris, France*
[14] *I. Physikalisches Institut, RWTH Aachen University, Aachen, Germany*
[15] *Fakultät Physik, Technische Universität Dortmund, Dortmund, Germany*
[16] *Max-Planck-Institut für Kernphysik (MPIK), Heidelberg, Germany*
[17] *Physikalisches Institut, Ruprecht-Karls-Universität Heidelberg, Heidelberg, Germany*
[18] *School of Physics, University College Dublin, Dublin, Ireland*
[19] *INFN Sezione di Bari, Bari, Italy*
[20] *INFN Sezione di Bologna, Bologna, Italy*
[21] *INFN Sezione di Ferrara, Ferrara, Italy*
[22] *INFN Sezione di Firenze, Firenze, Italy*
[23] *INFN Laboratori Nazionali di Frascati, Frascati, Italy*
[24] *INFN Sezione di Genova, Genova, Italy*
[25] *INFN Sezione di Milano, Milano, Italy*
[26] *INFN Sezione di Milano-Bicocca, Milano, Italy*
[27] *INFN Sezione di Cagliari, Monserrato, Italy*
[28] *Universita degli Studi di Padova, Universita e INFN, Padova, Padova, Italy*
[29] *INFN Sezione di Pisa, Pisa, Italy*

[30] *INFN Sezione di Roma La Sapienza, Roma, Italy*
[31] *INFN Sezione di Roma Tor Vergata, Roma, Italy*
[32] *Nikhef National Institute for Subatomic Physics, Amsterdam, Netherlands*
[33] *Nikhef National Institute for Subatomic Physics and VU University Amsterdam, Amsterdam, Netherlands*
[34] *AGH — University of Science and Technology, Faculty of Physics and Applied Computer Science, Kraków, Poland*
[35] *Henryk Niewodniczanski Institute of Nuclear Physics Polish Academy of Sciences, Kraków, Poland*
[36] *National Center for Nuclear Research (NCBJ), Warsaw, Poland*
[37] *Horia Hulubei National Institute of Physics and Nuclear Engineering, Bucharest-Magurele, Romania*
[38] *Petersburg Nuclear Physics Institute NRC Kurchatov Institute (PNPI NRC KI), Gatchina, Russia*
[39] *Institute for Nuclear Research of the Russian Academy of Sciences (INR RAS), Moscow, Russia*
[40] *Institute of Nuclear Physics, Moscow State University (SINP MSU), Moscow, Russia*
[41] *Institute of Theoretical and Experimental Physics NRC Kurchatov Institute (ITEP NRC KI), Moscow, Russia*
[42] *Yandex School of Data Analysis, Moscow, Russia*
[43] *Budker Institute of Nuclear Physics (SB RAS), Novosibirsk, Russia*
[44] *Institute for High Energy Physics NRC Kurchatov Institute (IHEP NRC KI), Protvino, Russia, Protvino, Russia*
[45] *ICCUB, Universitat de Barcelona, Barcelona, Spain*
[46] *Instituto Galego de Física de Altas Enerxías (IGFAE), Universidade de Santiago de Compostela, Santiago de Compostela, Spain*
[47] *Instituto de Fisica Corpuscular, Centro Mixto Universidad de Valencia — CSIC, Valencia, Spain*
[48] *European Organization for Nuclear Research (CERN), Geneva, Switzerland*
[49] *Institute of Physics, Ecole Polytechnique Fédérale de Lausanne (EPFL), Lausanne, Switzerland*
[50] *Physik-Institut, Universität Zürich, Zürich, Switzerland*
[51] *NSC Kharkiv Institute of Physics and Technology (NSC KIPT), Kharkiv, Ukraine*
[52] *Institute for Nuclear Research of the National Academy of Sciences (KINR), Kyiv, Ukraine*
[53] *University of Birmingham, Birmingham, United Kingdom*
[54] *H.H. Wills Physics Laboratory, University of Bristol, Bristol, United Kingdom*
[55] *Cavendish Laboratory, University of Cambridge, Cambridge, United Kingdom*
[56] *Department of Physics, University of Warwick, Coventry, United Kingdom*
[57] *STFC Rutherford Appleton Laboratory, Didcot, United Kingdom*
[58] *School of Physics and Astronomy, University of Edinburgh, Edinburgh, United Kingdom*
[59] *School of Physics and Astronomy, University of Glasgow, Glasgow, United Kingdom*
[60] *Oliver Lodge Laboratory, University of Liverpool, Liverpool, United Kingdom*
[61] *Imperial College London, London, United Kingdom*
[62] *Department of Physics and Astronomy, University of Manchester, Manchester, United Kingdom*
[63] *Department of Physics, University of Oxford, Oxford, United Kingdom*
[64] *Massachusetts Institute of Technology, Cambridge, MA, United States*
[65] *University of Cincinnati, Cincinnati, OH, United States*
[66] *University of Maryland, College Park, MD, United States*
[67] *Los Alamos National Laboratory (LANL), Los Alamos, United States*
[68] *Syracuse University, Syracuse, NY, United States*
[69] *School of Physics and Astronomy, Monash University, Melbourne, Australia, associated to* [56]
[70] *Pontifícia Universidade Católica do Rio de Janeiro (PUC-Rio), Rio de Janeiro, Brazil, associated to* [2]
[71] *Physics and Micro Electronic College, Hunan University, Changsha City, China, associated to* [7]
[72] *Guangdong Provincial Key Laboratory of Nuclear Science, Guangdong-Hong Kong Joint Laboratory of Quantum Matter, Institute of Quantum Matter, South China Normal University, Guangzhou, China, associated to* [3]
[73] *School of Physics and Technology, Wuhan University, Wuhan, China, associated to* [3]

JHEP05(2022)038

[74] Departamento de Fisica, Universidad Nacional de Colombia, Bogota, Colombia, associated to [13]
[75] Universität Bonn — Helmholtz-Institut für Strahlen und Kernphysik, Bonn, Germany, associated to [17]
[76] Institut für Physik, Universität Rostock, Rostock, Germany, associated to [17]
[77] Eotvos Lorand University, Budapest, Hungary, associated to [48]
[78] INFN Sezione di Perugia, Perugia, Italy, associated to [21]
[79] Van Swinderen Institute, University of Groningen, Groningen, Netherlands, associated to [32]
[80] Universiteit Maastricht, Maastricht, Netherlands, associated to [32]
[81] National Research Centre Kurchatov Institute, Moscow, Russia, associated to [41]
[82] National Research University Higher School of Economics, Moscow, Russia, associated to [42]
[83] National University of Science and Technology "MISIS", Moscow, Russia, associated to [41]
[84] National Research Tomsk Polytechnic University, Tomsk, Russia, associated to [41]
[85] DS4DS, La Salle, Universitat Ramon Llull, Barcelona, Spain, associated to [45]
[86] Department of Physics and Astronomy, Uppsala University, Uppsala, Sweden, associated to [59]
[87] University of Michigan, Ann Arbor, United States, associated to [68]

[a] Universidade Federal do Triângulo Mineiro (UFTM), Uberaba-MG, Brazil
[b] Hangzhou Institute for Advanced Study, UCAS, Hangzhou, China
[c] Excellence Cluster ORIGINS, Munich, Germany
[d] Università di Bari, Bari, Italy
[e] Università di Bologna, Bologna, Italy
[f] Università di Cagliari, Cagliari, Italy
[g] Università di Ferrara, Ferrara, Italy
[h] Università di Firenze, Firenze, Italy
[i] Università di Genova, Genova, Italy
[j] Università degli Studi di Milano, Milano, Italy
[k] Università di Milano Bicocca, Milano, Italy
[l] Università di Modena e Reggio Emilia, Modena, Italy
[m] Università di Padova, Padova, Italy
[n] Scuola Normale Superiore, Pisa, Italy
[o] Università di Pisa, Pisa, Italy
[p] Università della Basilicata, Potenza, Italy
[q] Università di Roma Tor Vergata, Roma, Italy
[r] Università di Urbino, Urbino, Italy
[s] MSU — Iligan Institute of Technology (MSU-IIT), Iligan, Philippines
[t] P.N. Lebedev Physical Institute, Russian Academy of Science (LPI RAS), Moscow, Russia
[u] Novosibirsk State University, Novosibirsk, Russia

[†] Deceased